Journal of Photochemistry and Photobiology A: Chemistry 202 (2009) 122–127

Contents lists available at ScienceDirect

Journal of Photochemistry and Photobiology A: Chemistry

journal homepage: www.elsevier.com/locate/jphotochem

First-principle studies on the exceptionally active triplet oxygen species in microporous zeolite materials: Reservation and catalysis

Gang Yang[a,b,*], Jing Guan[a], Lijun Zhou[b], Xianchun Liu[a], Xiuwen Han[a], Xinhe Bao[a,**]

[a] *State Key Laboratory of Catalysis, Dalian Institute of Chemical Physics, Chinese Academy of Sciences, 457 Zhongshan Road, Dalian 116023, PR China*
[b] *Key Laboratory of Forest Plant Ecology, Northeast Forestry University, Ministry of Education, Harbin 150040, PR China*

ARTICLE INFO

Article history:
Received 10 March 2008
Received in revised form
16 September 2008
Accepted 1 December 2008
Available online 11 December 2008

Keywords:
Density functional
Methane oxidation
Reservation
Triplet oxygen species
Zeolite catalysis

ABSTRACT

Density functional theory calculations were used to explore the reservation and catalytic properties of the exceptionally active triplet oxygen species in microporous ZSM-5 zeolite. It was found that the triplet oxygen species in H-form ZSM-5 zeolite can be reserved in the form of the more stable singlet oxygen species commonly found in solid-state materials, and moreover the single oxygen species is facile to be photolyzed into the triplet oxygen species without destructions to zeolite frameworks. It thus provides a route to store the triplet oxygen species ready for catalytic uses. On the contrary, the metal-exchanged ZSM-5 zeolites are proven to be unsuitable reservoirs to the triplet oxygen species due to the comparable instability of the singlet species. The activation barrier of methane hydroxylation catalyzed by the triplet oxygen species in H-form ZSM-5 zeolite was calculated to be 7.12 kcal mol^{-1}, which is much lower than that in Fe-exchanged ZSM-5 zeolite and will proceed at room temperature. Combined with the previous results, it was shown that the triplet oxygen species anchored by the isolated Brönsted acidic sites in H-form ZSM-5 zeolite are potentially excellent oxidants for varieties of important processes.

1. Introduction

Owing to its excellent performance in a variety of oxidation processes, the active triplet oxygen species O(^{3}P) has recently received increasing attention from both experimental and theoretical aspects [1–10]. The reaction process between the triplet oxygen species O(^{3}P) and CH_3Cl was monitored and evidenced by the infrared spectroscopic technique, and combined with the *ab initio* calculations the structures and vibrational spectrum of CH_3ClO singlet and $CH_3Cl\cdots O$ triplet were resolved [2]. Using quantum Monte Carlo and density functional theory, Grossman et al. [4] revealed that the triplet oxygen species O(^{3}P) is an effective oxidant for the reaction of cyclopentadiene conversion into 2-cyclopenenone and 3-cyclopentenone. As is well-known to us, the selective oxidation of light alkanes such as methane and propane represents one of today's biggest challenges [11,12]. The recent studies [3,8,9] showed that triplet oxygen species O(^{3}P) plays an important role in this research area. Tanner et al. [3] found that the microwave irradiation of the He/O_2 mixture generated the triplet oxygen species, which reacts efficiently with olefins to produce epoxides or aldehydes. The liquid-phase photolysis of 1,2-benzodiphenylene sulfoxide or dibenzothiophene sulfoxide can also generate the triplet oxygen species [9]. The sulfoxide photochemistry was rationalized with the primary formation of the triplet oxygen species in which the charge-transfer interaction between the triplet oxygen species and substrates (e.g., alkanes) preceded the oxidation process. The acyclic alkanes were found efficiently hydroxylated by the triplet oxygen species, whose reaction activity was compared with ozone (O_3) [8].

To best of our knowledge, effective methods are much lacking as to how to reserve and store the triplet oxygen species due to its exceptionally high activity. It thus seriously hampers the further researches and applications. Zeolites are an important class of industrial materials used throughout the petroleum refining, petrochemical and chemical industries. A good example is microporous zeolite ZSM-5, developed by Mobil Oil [13], is an aluminosilcate with high Si/Al ratios [14,15]. Previously, the present authors [16] found that the singlet N_2O molecules at the Brönsted acidic sites of ZSM-5 zeolite can be photolyzed into the triplet state and meanwhile release the triplet oxygen species which was anchored by the Brönsted acidic sites. The produced triplet oxygen species is capable of oxidizing CO into CO_2. In the present work, the effective reservation method of the exceptionally active triplet oxygen species in solid-state materials (e.g., ZSM-5 zeolite) was explored by first-principle calculations; i.e., in the form of the singlet state commonly found in solid-state materials. Note that the reserved singlet oxygen species should be facile to be

---

[*] Corresponding author at: State Key Laboratory of Catalysis, Dalian Institute of Chemical Physics, Chinese Academy of Sciences, 457 Zhongshan Road, Dalian 116023, PR China. Tel.: +86 411 84379528; fax: +86 411 84694447.
[**] Corresponding author.
E-mail addresses: dicpyanggang@yahoo.com.cn (G. Yang), xhbao@dicp.ac.cn (X. Bao).

1010-6030/$ – see front matter © 2008 Elsevier B.V. All rights reserved.
doi:10.1016/j.jphotochem.2008.12.010

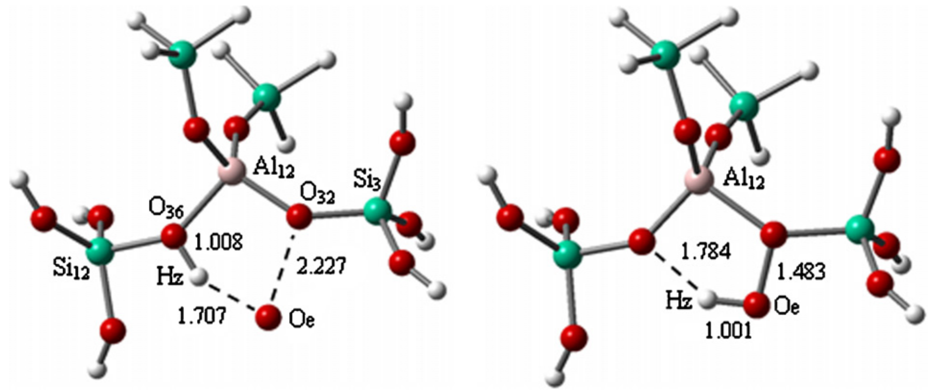

(a) $O(^3P)$-5T (b) $O(^1S)$-5T

Fig. 1. 5T clusters representing the H-ZSM-5 zeolite with the triplet and singlet oxygen species adsorbed at the Brönsted acidic sites. (a) $O(^3P)$-5T and (b) $O(^1S)$-5T.

revived to form the active triplet oxygen species ready for catalytic uses. With the catalytic triplet oxygen species in ZSM-5 zeolite, the C–H activation process of methane (CH_4) was investigated. On such basis, the potential applications of the triplet oxygen species in ZSM-5 zeolite were discussed by comparing its reaction activity with the current Fe-ZSM-5 zeolite catalysts.

2. Computational details

2.1. Cluster models

To study the dependence of theoretical results on cluster sizes, three different cluster models were employed in this work: (1) 5T cluster model (5T, see Fig. 1). This cluster model was used in our previous zeolite calculations and obtained reliable results [17–19]. The boundary Si and O atoms were saturated by H atoms, which were oriented in the direction of what would normally be the next framework atoms. The corresponding Si–H and O–H distances were altered to 1.500 and 1.000 Å, respectively. In order to retain the local structure of ZSM-5 zeolite, the boundary Si and O atoms were fixed in their crystallographic positions. (2) 7T cluster model (7T, see Fig. 2) [16]. This cluster model was larger than 5T cluster model and the boundary atoms were treated in the same way as in 5T cluster model. (3) Embedded cluster model (Em, see Fig. 3). This cluster model is much larger in size than 5T and 7T cluster models. The Em cluster contains altogether 25T sites and a complete 10-membered straight channel. The $(OSiO_3)_2Al(OSiH_3)_2$ fragment was designated as the active site of H-form ZSM-5 zeolite (H-ZSM-5) whereas the rest as the environment. Analogous to the 5T and 7T cluster models, the boundary Si and O atoms were saturated by H atoms, which were oriented in the direction of what would normally be the next framework atoms; the corresponding Si–H and O–H distances were altered to 1.500 and 1.000 Å, respectively. Except for the environmental atoms, all the atoms including the adsorbents were fully relaxed during the geometry optimizations.

2.2. Theoretical methods

First principles density functional calculations were performed using the B3LYP functional [20,21] under Gaussian 98 program [22]. The B3LYP method has been proven to be reliable to treat the excited states [23–26]. The transition states were determined using the Synchronous Transit Quasi Newton (STQN) technique, followed by frequency calculations to ensure that only one imaginary vibration corresponds to the transition state. The 6-31G(d) basis set was used to describe the 5T, 7T, the active sites of the Em cluster model as well as the adsorbents (e.g., the triplet and singlet oxygen species as well as the methane molecule). As to the environmental atoms in the Em cluster model, they were treated with 3-21G basis set.

3. Results and discussion

3.1. $O(^3P)$ and $O(^1S)$ at the acidic site of H-ZSM-5 zeolite

As described in Computational details, the adsorption of the triplet and singlet oxygen species at the acidic sites of H-ZSM-5

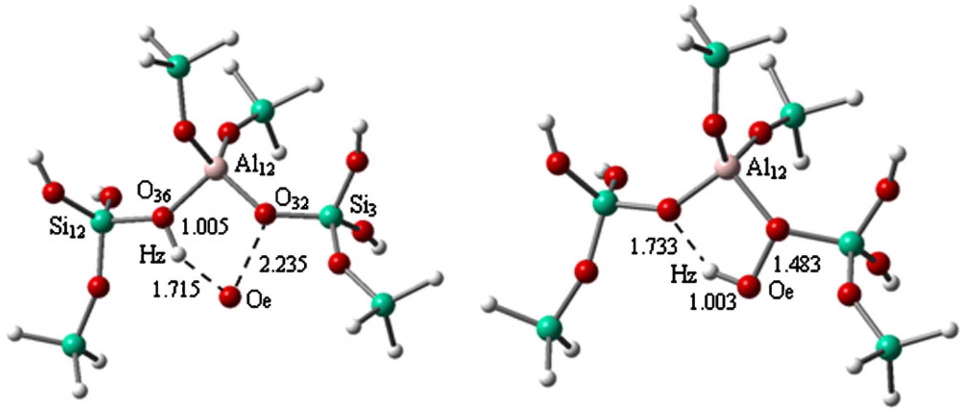

(a) $O(^3P)$-7T (b) $O(^1S)$-7T

Fig. 2. 7T clusters representing the H-ZSM-5 zeolite with the triplet and singlet oxygen species adsorbed at the Brönsted acidic sites. (a) $O(^3P)$-7T and (b) $O(^1S)$-7T.

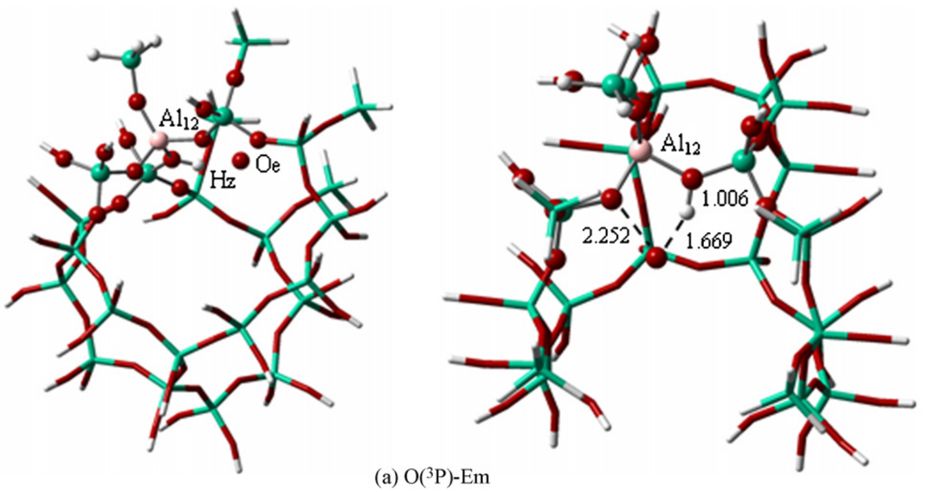

(a) $O(^3P)$-Em

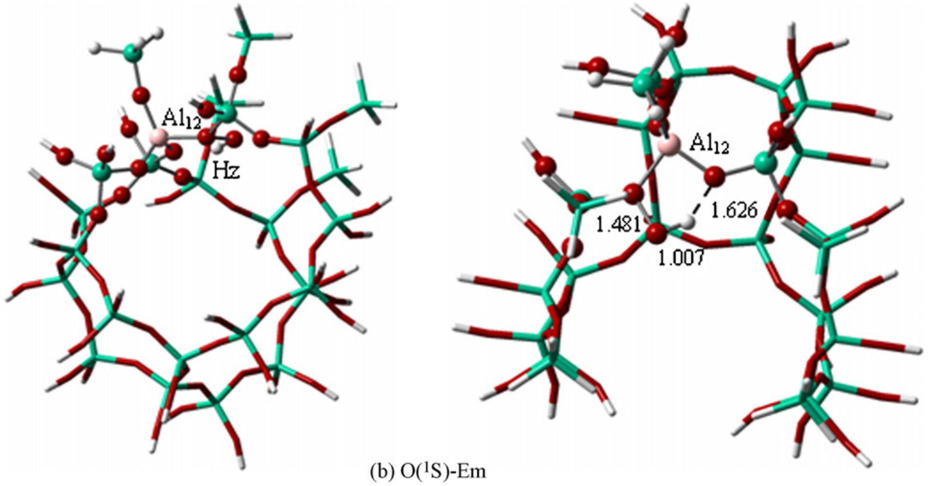

(b) $O(^1S)$-Em

Fig. 3. Em clusters of H-ZSM-5 zeolite adsorbed with the triplet and singlet oxygen species. Presentations along the straight channel (one the left) and zigzag channel (on the right), respectively. (a) $O(^3P)$-Em and (b) $O(^1S)$-Em.

zeolite was studied by three different cluster models, see Figs. 1–3. Some distances of 5T and 7T clusters were given in Figs. 1 and 2, respectively, from where it can be found that the geometric parameters of these two cluster models are rather close to each other. Accordingly, 5T and 7T cluster models are comparable to obtain reliable results. The H_z–O_{36} bond in $O(^3P)$-7T (Fig. 2(a)) was optimized to be 1.005 Å, slightly elongated than the distance of 0.974 Å in H-ZSM-5 zeolite [16]. It was caused by the formation of strong hydrogen bonding of H_z–O_e with the distance equalling 1.715 Å. The O_e–O_{32} distance was calculated at 2.235 Å in $O(^3P)$-7T, indicating that these two O atoms show attractions instead of repulsions towards each other, or else the O_e atom will be pushed far away from the O_{32} atom at the acidic site. In addition, the adsorption energies of the triplet oxygen species on the 5T and 7T clusters were computed to be −11.17 and −11.29 kcal mol^{-1}, respectively. It is obvious that the H_z–O_{36} hydrogen bond alone is not sufficient to cause such large adsorption energies, thus confirming the attractive interactions present between the O_e and O_{32} atoms. The spin density (S_d) was found primarily localized on the O_e atom ($S_d = 1.84$), with the rest distributed to the O_{32} atom ($S_d = 0.17$). As to the singlet oxygen species in H-ZSM-5 zeolite (Figs. 1(b) and 2(b)), the acidic H_z atom is bonded with the O_e atom instead of the lattice O_{32} atom as in the case of the triplet oxygen species. The H_z–O_e bond lengths are equal to 1.003 Å in $O(^1S)$-7T. The H_z–O_{36} distance was optimized at 1.733 Å in $O(^1S)$-7T, suggesting that these two atoms are no longer bonded. Instead, direct bond was found to have formed between the O_e and O_{32} atoms. Its distance was optimized to be 1.483 Å in $O(^1S)$-7T, very close to the O–O distance of 1.480 Å in the binuclear iron peroxide species in TS-1 and Fe/ZSM-5 zeolite [19,27,28]. That is, the HO_2^- peroxide species was formed in $O(^1S)$-7T.

Fig. 3(a) and (b) shows the two-layer embedded (Em) clusters adsorbed with the triplet and singlet oxygen species, respectively. In consistency with the 5T and 7T results, the acidic H_z atom forms direct bond with the O_{36} atom and hydrogen bond with the O_e atom in $O(^3P)$-Em whereas in the reverse situations in $O(^1S)$-Em. Moreover, direct O_e–O_{32} bond was formed in the case of $O(^1S)$-Em with its distance optimized at 1.481 Å. The Em distances are rather close to those of 5T and 7T clusters except the O_{36}–H_z distance where the deviation between the Em and 5T/7T clusters amounts to 0.158/0.107 Å. Albeit this deviation, the geometries of the active sites in Em clusters can be regarded to resemble those of 5T and 7T clusters, see Figs. 1–3.

3.2. *The reservation of the triplet oxygen species in H-ZSM-5 zeolite*

The energy difference between the triplet and singlet oxygen species was defined as $E_d = E[O(^3P)] - E[O(^1S)]$. For 5T, 7T and Em clusters, the E_d values were calculated at 17.04, 18.85, 16.08 kcal mol^{-1}, respectively, agreeing with the geometric data that the results of the three cluster models are close to each other. The singlet oxygen species in H-ZSM zeolite was found to be lower in energy and thus more stable than the triplet oxygen species. In gas phase; i.e., in the absence of zeolites, the E_d value was

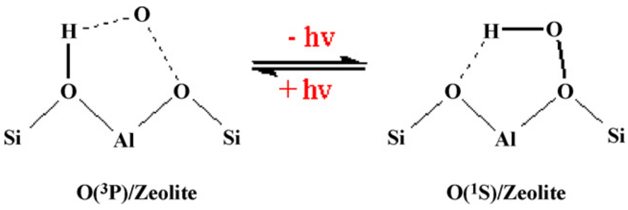

Scheme 1. Interconversions between the triplet and singlet oxygen species in H-ZSM-5 zeolite.

calculated to be $-64.77\,\mathrm{kcal\,mol^{-1}}$, which is consistent with the fact that the ground state of the oxygen atom in gas phase is the triplet. However, the presence of H-ZSM-5 zeolite reverses the sequence of the relative stabilities of the gas-phase singlet and triplet oxygen species and greatly enhances the stability of the singlet oxygen species, the predominant oxygen species found in solid-state materials. In H-ZSM-5 zeolite, the singlet oxygen species is now favoured over the triplet oxygen species and becomes the ground state for the oxygen atom, which may be the prerequisite to be reserved in solid-state materials such as H-ZSM-5 zeolite. Moreover, the geometry-optimization processes indicated that the quench of the radical in $O(^3P)$-7T will gradually evolve into $O(^1S)$-7T and the excitation of $O(^1S)$-7T will gradually lead to the formation of $O(^3P)$-7T. Therefore, the triplet and singlet oxygen species in H-ZSM-5 zeolite can be interconverted, as represented by Scheme 1. The triplet oxygen species in H-ZSM-5 zeolite is ready to be quenched into the singlet state, which is the common and stable oxygen species in solid-state materials. It thus provides a route to store the exceptionally triplet oxygen species.

In 7T clusters, the wavelength for the excitation of triplet and singlet oxygen was calculated to be 1517.8 nm. It corresponds to the vibrational frequency of $6586.7\,\mathrm{cm^{-1}}$. All the calculated lattice vibrations of zeolites were found to be below $1200.0\,\mathrm{cm^{-1}}$, in agreement with the experimental results [29–31]. In addition, the vibration of $6586.7\,\mathrm{cm^{-1}}$ is also far beyond the hydroxyl vibrations of Brönsted acidic sites and defect sites [32,33]. Accordingly, the excitation of the singlet oxygen species in H-ZSM-5 zeolite will not bring about destructions to the zeolite frameworks, which ensures the effective excitations of the singlet oxygen species in H-ZSM-5 zeolite and the cyclic utilizations of zeolite catalysts.

3.3. $O(^3P)$ and $O(^1S)$ in Na-ZSM-5 zeolite

Fig. 4 depicted the triplet and singlet oxygen species in Na-exchanged ZSM-5 zeolite. Before adsorption, the $Na–O_{36}$ and $Na–O_{32}$, $Na–O_{32}{}^*$ and $Na–O_{14}$ distances were optimized at 2.176, 2.255, 2.953 and 3.632 Å, and due to the $O(^3P)$ adsorption (Fig. 4(a)) these distances change slightly with their exact values of 2.199, 2.278, 2.986 and 3.601 Å, respectively. Note that the asterisk in $Na–O_{32}{}^*$ was used to differentiate the two O_{32} atoms, see the details in Fig. 4(a). It indicates that the adsorption of the triplet oxygen species exerts an inconspicuous influence on the geometry of Na-ZSM-5 zeolite. In $O(^3P)$-Na-7T (Fig. 4(a)), the O_e atom forms direct bond with the Na ion. In agreement with the $O(^3P)$-7T results, the spin density (S_d) is mainly localized on the O_e atom ($S_d = 1.85$), with the rest on another lattice oxygen atom of O_{14} ($S_d = 0.17$). In $O(^1S)$-Na-7T (Fig. 4(b)), the $Na–O_{36}$ and $Na–O_{32}$, $Na–O_{32}{}^*$ and $Na–O_{14}$ distances were optimized at 2.362, 2.219, 3.348 and 3.266 Å, respectively, showing noticeable differences from the values in $O(^3P)$-Na-7T. The $O_e–O_{14}$ distance was remarkably shortened from 2.313 Å in $O(^3P)$-Na-7T to 1.528 Å in $O(^1S)$-Na-7T, indicating that direct $O_e–O_{14}$ bond has formed in the case of the $O(^1S)$ species. However, the distances showed that the interaction between the O_e and O_{32} atoms in H-ZSM-5 zeolite is stronger than that between the O_e and O_{14} atoms in Na-exchanged ZSM-5 zeolite.

Albeit the formation of the direct $Na–O_e$ bond in $O(^3P)$-Na-7T, the adsorption energy of the triplet oxygen species amounts to $-11.31\,\mathrm{kcal\,mol^{-1}}$ and is much lower than expected. The superficial geometries of $O(^3P)$-Na-7T and $O(^1S)$-Na-7T are alike to each other, as deduced from the structures shown in Fig. 4(a) and (b). The geometry-optimization procedures indicated that the triplet and singlet oxygen species in Na-exchanged ZSM-5 zeolite can be interconverted just as the situations in H-form zeolite. However, the relative stability of the singlet oxygen species over the triplet oxygen species has not been improved at all in Na-exchanged ZSM-5 zeolite, for $O(^1S)$-Na-7T was calculated even slightly higher in energy than $O(^3P)$-Na-7T with the energy of $0.47\,\mathrm{kcal\,mol^{-1}}$. Accordingly, the exceptionally active triplet oxygen species cannot be reserved in form of the singlet oxygen species in Na-exchanged zeolites but can in H-form zeolites.

3.4. Activation of the C–H bond in methane by $O(^3P)$ in ZSM-5 zeolite

Upon methane (CH_4) adsorption, the geometries of the CH_4 and $O(^3P)$-7T fragments remain almost intact, and the two shortest $(H_3C–)H–O_e$ distances were optimized at 2.837 and 3.055 Å, respectively, see CH_4–$O(^3P)$-7T in Fig. 5(a). In addition, the spin densities (S_d) on the O_e and O_{32} atoms in CH_4–$O(^3P)$-7T are equal to 1.84 and 0.17, respectively, exactly identical to the values in $O(^3P)$-7T. As expected, the adsorption energy of methane on $O(^3P)$-7T is very

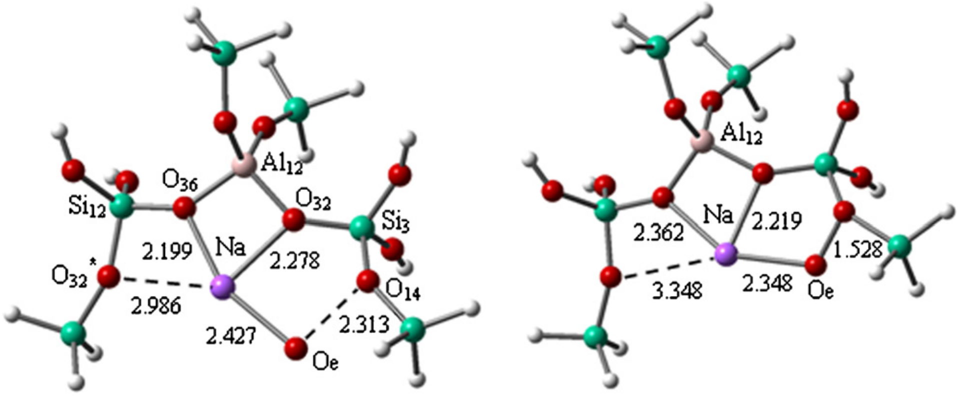

(a) $O(^3P)$-Na-7T (b) $O(^1S)$-Na-7T

Fig. 4. 7T clusters representing the Na-exchanged ZSM-5 zeolite with adsorption of the triplet and singlet oxygen species. (a) $O(^3P)$-Na-7T and (b) $O(^1S)$-Na-7T.

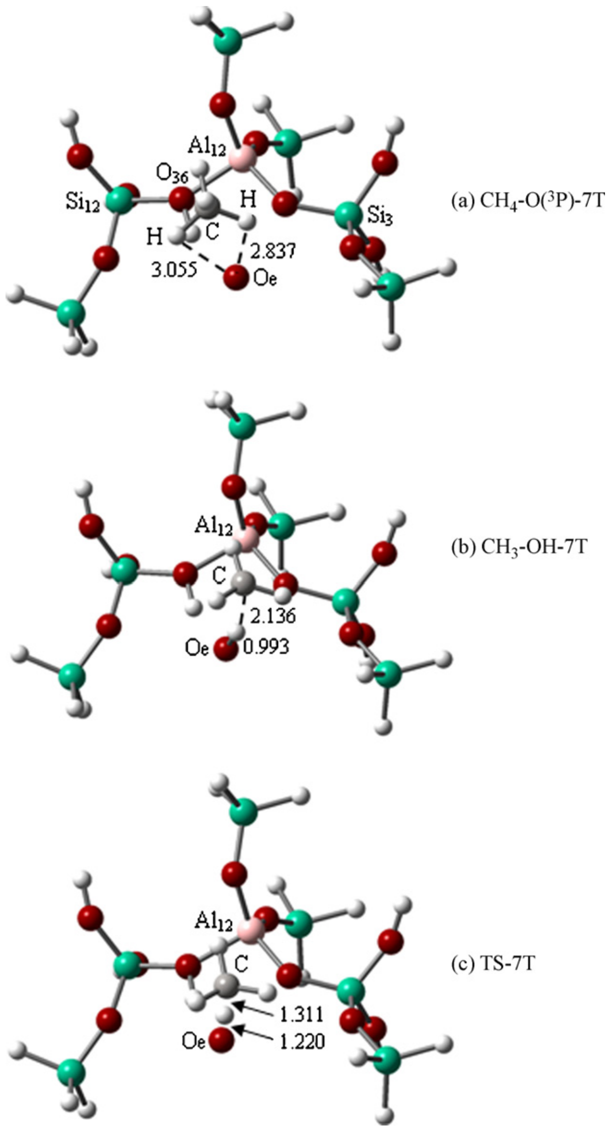

(a) CH_4-$O(^3P)$-7T

(b) CH_3-OH-7T

(c) TS-7T

Fig. 5. The structures of reactant, product and transition state (TS) for the H-abstraction reaction in methane catalyzed by $O(^3P)$/H-ZSM-5 zeolite. (a) CH_4–$O(^3P)$-7T, (b) CH_4–OH-7T, and (c) TS-7T.

slight and was calculated to be −1.25 kcal mol^{-1}. The product of the H-abstraction process (CH_3–OH-7T) was shown in Fig. 5(b), where one H atom of methane was transferred to the O_e atom of the $O(^3P)$-7T fragment. The C–H and H–O_e distances were optimized at 2.136 and 0.993 Å, respectively. The spin densities (S_d) are distributed mainly on the O_e and C atoms with the exact values of 0.95 and 1.07, respectively, different from the situations in $O(^3P)$-7T or CH_4–$O(^3P)$-7T where the spin densities are mainly localized on the O_e atom. The transition state structure was determined and shown in Fig. 5(c), which is characterized by the only imaginary frequency at −1338.37 cm^{-1}. The activation barrier of the H-abstraction reaction in methane was calculated to be 7.12 kcal mol^{-1}, which is small enough to be easily crossed over at room temperatures. The formation of the Fe–OH species in methane adsorbed Fe/ZSM-5 zeolite systems requires an activation barrier over 30.0 kcal mol^{-1} [34–36]. Accordingly, the triplet oxygen species $O(^3P)$ in microporous zeolites will greatly lower the energy barrier of the C–H activation in methane. Moreover, the isolated Brönsted acidic sites in H-ZSM-5 zeolite will restrict the further oxidation of methane to a certain degree and meanwhile offer an ideal locale for the catalytic processes to take place [16].

4. Conclusions

This work reported a density functional theory investigation on the reservation and catalytic properties of the exceptionally active triplet oxygen species in solid-state materials. The microporous ZSM-5 zeolite was used as the exemplified solid-state materials due to its wide application in catalytic aspects.

The triplet and singlet oxygen species in H-ZSM-5 zeolite can be interconverted. In H-ZSM-5 zeolite, the singlet oxygen species is the ground state and lower by ca. 17.0 kcal mol^{-1} than the triplet oxygen species, quite different from the situations in gas phase where the triplet oxygen species is the ground state and preferred by 64.77 kcal mol^{-1}. It indicates that the triplet oxygen species in H-ZSM-5 zeolite can be reserved in the form of the singlet oxygen species commonly found in solid-state materials. The HO_2^- peroxide species was formed in the singlet oxygen species adsorbed H-ZSM-5 zeolite. Moreover, the excitation of the singlet oxygen species to the triplet oxygen species will not bring about destructions to the zeolites, thus providing a practical route to store and reserve the exceptionally triplet oxygen species.

In Na-exchanged ZSM-5 zeolite, the triplet and singlet oxygen species can be interconverted as well. However, the singlet oxygen species is slightly higher in energy than the triplet oxygen species, suggesting that the metal-exchanged zeolites may not be the suitable reservoirs to store the exceptionally triplet oxygen species in the form of the singlet species.

Methane is facile to be hydroxylated in H-ZSM-5 zeolite, with the activation barrier much lower than the currently focused catalysts of Fe-ZSM-5 zeolite. Combined with the previous results of CO oxidation [16], it was found that the triplet oxygen species at the isolated Brönsted acidic sites in H-ZSM-5 zeolite are excellent oxidant to varieties of important reactions.

Acknowledgments

We gratefully acknowledge the financial support of the National Natural Science Foundation of China (No. 20403017), the Talented Funds of Northeast Forestry University (No. 220-602042) and Chinese Postdoc Foundation (No. 20060400802).

References

[1] A.C. Knipe, W.E. Watts (Eds.), Organic Reaction Mechanisms, John Wiley & Sons Inc., 1998, pp. 217–253.
[2] L. Schriver-Mazzuoli, A. Schriver, Y. Hannachi, J. Phys. Chem. A 102 (1998) 10221–10229.
[3] D.D. Tanner, P. Kandanarachchi, N.C. Das, M. Brausen, C.T. Vo, D.M. Camaioni, J.A. Franz, J. Org. Chem. 63 (1998) 4587–4593.
[4] J.C. Grossman, W.A. Lester Jr., S.G. Louie, J. Am. Chem. Soc. 122 (2000) 705–711.
[5] J.P. Reid, C.X.W. Qian, S.R. Leone, Phys. Chem. Chem. Phys. 2 (2000) 853–860.
[6] G. Li, S.B.M. Bosio, W.L. Hase, J. Mol. Struct. 556 (2000) 43–57.
[7] D. Hodgson, H.Y. Zhang, M.R. Nimlos, J.T. Mckinnon, J. Phys. Chem. A 105 (2001) 4316–4327.
[8] E. Zadok, Y. Mazur, Angew. Chem. Int. Ed. 21 (1982) 303.
[9] K.B. Thomas, A. Greer, J. Org. Chem. 68 (2003) 1886–1891.
[10] G.D. DeBoer, J.A. Dodd, J. Phys. Chem. A 111 (2007) 12977–12984.
[11] C.G. Jia, T. Kitamura, Y. Fujiwara, Acc. Chem. Res. 34 (2001) 633–639.
[12] S. Feyel, J. Döbler, D. Schröder, J. Sauer, H. Schwarz, Angew. Chem. Int. Ed. 45 (2006) 4677–4681.
[13] G.T. Kokotailo, S.L. Lawton, D.H. Olson, W.M. Meier, Nature 272 (1978) 437–438.
[14] E. Roduner, H. Dilger, J. Am. Chem. Soc. 123 (2001) 7717–7718.
[15] A. Zecchina, M. Rivallan, G. Berlier, C. Lamberti, G. Ricchiardi, Phys. Chem. Chem. Phys. 9 (2007) 3483–3499.
[16] G. Yang, J. Guan, L.J. Zhou, X.C. Liu, X.W. Han, X.H. Bao, Micropor. Mesopor. Mater. 113 (2008) 583–587.
[17] G. Yang, D.H. Zhou, X.C. Liu, X.W. Han, X.H. Bao, J. Mol. Struct. 797 (2006) 131–139.
[18] G. Yang, L.J. Zhou, X.C. Liu, X.W. Han, X.H. Bao, J. Phys. Chem. B 110 (2006) 22295–22297.
[19] G. Yang, L.J. Zhou, X.C. Liu, X.W. Han, X.H. Bao, Catal. Commun. 8 (2007) 1981–1984.
[20] A.D. Becke, Phys. Rev. A 38 (1988) 3098–3100.
[21] C. Lee, W. Yang, R.G. Parr, Phys. Rev. B 37 (1988) 785–789.

[22] M.J. Frisch, G.W. Trucks, H.B. Schlegel, G.E. Scuseria, M.A. Robb, J.R. Cheeseman, V.G. Zakrzewski, J.A. Montgomery Jr., R.E. Stratmann, J.C. Burant, S. Dapprich, J.M. Millam, A.D. Daniels, K.N. Kudin, M.C. Strain, O. Farkas, J. Tomasi, V. Barone, M. Cossi, R. Cammi, B. Mennucci, C. Pomelli, C. Adamo, S. Clifford, J. Ochterski, G.A. Petersson, P.Y. Ayala, Q. Cui, K. Morokuma, D.K. Malick, A.D. Rabuck, K. Raghavachari, J.B. Foresman, J. Cioslowski, J.V. Ortiz, A.G. Baboul, B.B. Stefanov, G. Liu, A. Liashenko, P. Piskorz, I. Komaromi, R. Gomperts, R.L. Martin, D.J. Fox, T. Keith, M.A. Al-Laham, C.Y. Peng, A. Nanayakkara, C. Gonzalez, M. Challacombe, P.M.W. Gill, B. Johnson, W. Chen, M.W. Wong, J.L. Andres, C. Gonzalez, M. Head-Gordon, E.S. Replogle, J.A. Pople, Gaussian 98, Revision A.9, Gaussian Inc., Pittsburgh, PA, 1998.

[23] S. Nishida, K. Takahashi, Y. Matsumi, J. Phys. Chem. A 108 (2004) 2451–2456.

[24] X.J. Wang, W. Wang, M. Koyama, M. Kubo, A. Miyamoto, J. Photochem. Photobio. A: Chem. 179 (2006) 149–155.

[25] P.M. Esteves, B. Louis, J. Phys. Chem. B 110 (2006) 16793–16800.

[26] Y.J. Liu, L.D. Vico, R. Lindh, J. Photochem. Photobio. A: Chem. 194 (2008) 261–267.

[27] S. Bordiga, A. Damin, F. Bonino, G. Ricchiardi, C. Lamberti, A. Zecchina, Angew. Chem. Int. Ed. 41 (2002) 4734–4737.

[28] J.Q. Zhuang, G. Yang, G.D. Ma, X.J. Lan, X.M. Liu, X.W. Han, X.H. Bao, U. Müller, Angew. Chem. Int. Ed. 43 (2004) 6377–6381.

[29] E.M. Flanigen, H. Khatami, H.A. Seymenski, Adv. Chemistry Series 101, in: E.M. Flanigen, L.B. Sand (Eds.), American Chemical Society, Washington, DC, 1971, pp. 201–228.

[30] E. Geidel, H. Böhlig, Ch. Peuker, W. Pilz, Stud. Surf. Sci. Catalysis 65, in: G. Ohlmann, H. Pfeifer, R. Fricke (Eds.), Elsevier, Amsterdam, 1991, pp. 511–519.

[31] V.B. Kazansky, V.Y. Borovkov, H.G. Karge, J. Chem. Soc., Faraday Trans. 93 (1997) 1843–1848.

[32] E. Brunner, H.G. Karge, H. Pfeifer, Z. Phys. Chem. 176 (1992) 173–183.

[33] H.V. Brand, A. Redondo, P.J. Hay, J. Mol. Catal. A 121 (1997) 45–62.

[34] A.L. Yakovlev, G.M. Zhidomirov, R.A. van Santen, J. Phys. Chem. B 105 (2001) 12297–12302.

[35] K. Yoshizawa, Y. Shiota, T. Kamachi, J. Phys. Chem. B 107 (2003) 11404–11410.

[36] A. Heyden, B. Peters, A.T. Bell, F.J. Keil, J. Phys. Chem. B 109 (2005) 1857–1873.